SPECIAL TOPIC — 2D materials: physics and device applications

Geometric stability and electronic structure of infinite and finite phosphorus atomic chains*

Jingsi Qiao(乔婧思)†, Linwei Zhou(周霖蔚)†, and Wei Ji(季威)‡

Department of Physics and Beijing Key Laboratory of Optoelectronic Functional Materials & Micro-nano Devices, Renmin University of China, Beijing 100872, *China*

(Received 26 December 2016; revised manuscript received 3 February 2017; published online 15 February 2017)

One-dimensional mono- or few-atomic chains were successfully fabricated in a variety of two-dimensional materials, like graphene, BN, and transition metal dichalcogenides, which exhibit striking transport and mechanical properties. However, atomic chains of black phosphorus (BP), an emerging electronic and optoelectronic material, is yet to be investigated. Here, we comprehensively considered the geometry stability of six categories of infinite BP atomic chains, transitions among them, and their electronic structures. These categories include mono- and dual-atomic linear, armchair, and zigzag chains. Each zigzag chain was found to be the most stable in each category with the same chain width. The mono-atomic zigzag chain was predicted as a Dirac semi-metal. In addition, we proposed prototype structures of suspended and supported finite atomic chains. It was found that the zigzag chain is, again, the most stable form and could be transferred from mono-atomic armchair chains. An orientation dependence was revealed for supported armchair chains that they prefer an angle of roughly 35°–37° perpendicular to the BP edge, corresponding to the [110] direction of the substrate BP sheet. These results may promote successive research on mono- or few-atomic chains of BP and other two-dimensional materials for unveiling their unexplored physical properties.

Keywords: black phosphorus, atomic chain, Dirac semi-metal, one-dimension material

PACS: 68.65.–k, 81.07.Vb, 81.30.Dz **DOI:** 10.1088/1674-1056/26/3/036803

1. Introduction

With respect to the minimization of electronic and optoelectronic devices, the dimensionality of devices has been reducing from three-dimension to two-dimension (2D) and eventually to one-dimension (1D).[1–4] The ultimate small-size 1D devices are expected to be comprised of one or few-atoms width atomic chains which were realized in graphene, BN, and transition metal dichalcogenides (TMDs) by knocking out atoms from 2D nanosheets under electron beam irradiation.[5–9] These atomic chains were found of striking properties including excellent electric transport, high thermopower, and ultra-strong mechanical strength. Black phosphorus (BP), the most stable allotrope of phosphorus at ambient conditions, has attained tremendous attention since its rediscovery as a high-mobility, high thermo-power, anisotropic, and tunable direct bandgap semiconductor with dichroism optical response in 2014.[10–13] It is the very first elemental semiconductor in 2D layered materials with its bandgap covering near-infrared to visible light region.[11,14] It would be thus interesting if BP atomic chains could be realized in experiment and if these chains have any striking physical properties. Both of these questions are unknown and subject to further investigations.

In light of the experimental protocols adopted in the previous experiments,[15–17] a few-atom width ribbon is a precursor of mono-atomic chains, which could be fabricated by creating two parallel line defects apart by a few atoms. Recently, a theory predicted that a chain-like vacancy may form in BP nanosheets under electron irradiation, while similarline defects were observed in experiment during the period of summarizing this work.[18] Given these chain-like vacancies, the exact atomic structure of BP chains, the thermal stability and electronic structures of them are still unclear.

Here, we employ density functional theory (DFT) calculations to consider the likely structures of mono- and dual-atomic infinite and encapsulated finite BP chains. Three categories of mono-atomic infinite chains, namely, linear (L), armchair (AC), and zigzag (ZZ) chains, in addition with three associated categories of dual-atomic infinite chains, were considered in our calculations. It was found that zigzag chains are always energetically stable in both mono- and dual-atomic chains while linear chains are of the highest energies. Phase transitions among them were revealed relevant with the linear

*Project supported by the National Natural Science Foundation of China (Gant Nos. 11274380, 91433103, 11622437, and 61674171), the Fundamental Research Funds for the Central Universities, China, and the Research Funds of Renmin University of China (Grant No. 16XNLQ01). Qiao was supported by the Outstanding Innovative Talents Cultivation Funded Programs 2016 of Renmin University of China.

†These authors contributed equally to this work.

‡Corresponding author. E-mail: wji@ruc.edu.cn

© 2017 Chinese Physical Society and IOP Publishing Ltd

density of P atoms along the chain, as elucidated in a phase diagram. Electronic structures of these six chains were also discussed that a likely band inversion with spin–orbit coupling (SOC) was found in the infinite ZZ chain. Geometry and stability of finite chains were considered in models of a chain encapsulated in two BP half-sheets with and without the support from BP sheets underneath, which represent the most likely experimental cases.

2. Methods

Density functional theory calculations were performed using the generalized gradient approximation for the exchange–correlation potential, the projector augmented wave method,[19,20] and a plane wave basis set as implemented in the Vienna *ab-initio* simulation package (VASP)[21] and the quantum espresso (QE)[22] code. Density functional perturbation theory (DFPT)[23] was employed to calculate phonon dispersion relations using QE. In geometry optimization, van der Waals interactions were considered at the van der Waals density functional (vdW-DF)[24,25] level with the optB86b functional for the exchange potential (optB86b-vdW),[26,27] which was found more suitable than other vdW-DF functionals for modeling mechanical properties and interlayer coupling strength of 2D materials.[28–33] In terms of infinite chains, the energy cutoff for the plane-wave basis was set to 700 eV. A supercell containing only one (two) P atoms with vacuum regions of ~ 20 Å in the y and z directions was used to model the infinite linear (dual) atomic chain (Fig. 1(a)); while the supercells of AC and ZZ (dual) atomic chains were comprised of four and two (eight and four) P atoms, respectively (Figs. 1(b) and 1(c)). A k-mesh of $24\times1\times1$ was employed to sample the 1D Brillion zone (BZ) of infinite linear chains for both geometric and electronic structure calculations. The density of k points was kept fixed in sampling other infinite chains. For finite chains, a 9×3 supercell of BP monolayer, with lattice constants of $a = 40.57$ Å and $b = 9.97$ Å, was chosen to model both the BP half-sheets encapsulating the finite chains. The vacuum region was, again, ~ 20 Å in thickness. The kinetic energy cutoff for the plane-wave basis was set to 350 eV and a k-mesh of $1\times4\times1$ was adopted for finite chain calculations. Over 120 finite chains, with four edge geometries, namely, single-bond, 4-ring, 5-ring, and 6-ring, of the half-sheets.[34] and more than 9 chain orientations from [110] to [100], were considered. The shape and volume of the infinite supercells were fully relaxed until the residual force per atom and on the supercell was less than 0.001 eV/Å for infinite chains. In terms of finite chains, the shape and volume of the supercell were kept fixed but all atoms in it were fully relaxed until the residual force per atom was less than 0.01 eV/Å.

3. Results and discussion

3.1. Stability of infinite P chains

Figures 1(a)–1(c) show the side views of fully relaxed structures of three mono-atomic chains, denoted as m-L, m-ZZ, and m-AC. Their lattice constants along the x direction (a) are 2.13 Å, 3.14 Å, and 5.43 Å, respectively, however, those of dual-atomic chains (Figs. 1(d)–1(f)), denoted as d-L, d-ZZ, and d-AC, are 0.13 Å to 0.18 Å larger, i.e., 2.31 Å, 3.32 Å, and 5.56 Å, respectively. The enlarged lattice constant is primarily a result of the bond length elongation and the bond angle reduces by only 0.4° and 4.2° from 95.5° and 106.7° for ZZ and AC chains, respectively. The formation of one more P–P bonds in dual atomic chains reduces the electron density along the chain direction and thus weakens the P–P bond, leading to an enlarged bond length. Apparently, the supercells of these six infinite chains contain different numbers of P atoms, which hinders the direct comparison of their stability. We thus introduce a parameter, namely, the total energy normalized to each P atom (E_P). It explicitly indicates the order of stability as d-ZZ (-3.71eV) > d-AC (-3.64 eV) > m-ZZ (-3.46 eV) > m-AC (-3.37 eV) > d-L (-3.16 eV) > m-L (-2.67 eV). The linear chains are found very unstable that their energies are at least 0.5 eV higher than the ZZ and AC chains in the same category. Although the addition P–P bond in dual-atomic chains offers 0.25–0.27 eV lower energy, the energy difference between ZZ and AC chains is, however, rather small for either dual- (0.07 eV) or mono-atomic (0.09 eV) chains. These results indicate that keeping the P–P–P bond angle at roughly 100° is the key issue to stabilize the chains, as ascribed to the repulsion between two lone electron pairs of adjacent P atoms. Configuration d-ZZ (Fig. 1(f)) is the most stable one, but it is still 0.40 eV per P atom less stable than bulk BP. Phonon dispersion relation of m-ZZ was further checked to verify its stability, as plotted in Fig. 1(g). No imaginary frequency is found among the whole BZ, indicating that m-ZZ (Fig. 1(c)) should be stable at finite temperature. The frequency of the mode ZO is fairly low at the Γ point. Thus, the chain may break its high symmetry along the directions shown in the vibrational displacements (Fig. 1(h)). Infinite chains may undergo Peierls instability, forming a charge density wave. We thus doubled the size of the unit cell for each chain and broke the translational symmetry before structural relaxation. It shows that m- or d-ZZ chain is rather robust and all m- or d-ZZ structures with broken symmetry are relaxed back to keep the original form. However, m-AC chains may undergo a phase transition transferring to d-ZZ chains if the volume of the cell is not restricted.

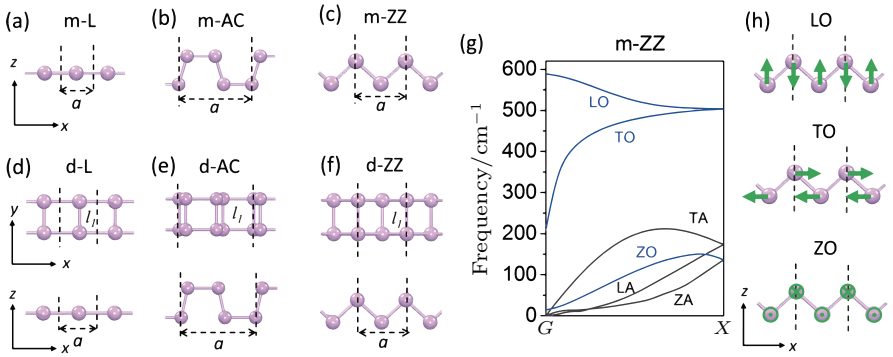


Fig. 1. (color online) Geometric stucutres of six representative 1D infinite atomic chains: (a) mono-linear chain (L), (b) mono-armchair chain (AC), (c) mono-zigzag chain (ZZ), (d) dual-linear chain (d-L), (e) dual-armchair chain (d-DB), (f) dual-zigzag chain (d-ZZ). Lattice constant a is marked on each configuration. Bond lengths l_1 of dual-chains are labeled in panels (d)–(f). (g) Phonon dispersion relation of the m-ZZ chain. (h) Vibrational displacements for three optical modes of the m-ZZ chain.

3.2. Structural phase transition among infinite chains

These six infinite chains are transferable by stretching or compressing them along the infinite direction. It thus requires a parameter describing the relationship between length and energy. Here, we introduce a geometric parameter (n) which represents the length, in units of Å, of each P atom in a chain. The n values, the inversion of linear density of P atoms, are 2.13 Å, 1.57 Å, and 1.36 Å for m-L, m-ZZ, and m-AC, respectively, while those n values for the dual-atomic chains are almost one-half of the corresponding values of the mono-atomic chains, i.e., 1.15 Å, 0.83 Å, and 0.70 Å, respectively. A phase diagram was plotted by recording energy evolution of different chains during elongation and contraction, as shown in Fig. 2. It explicitly shows a reversible phase transition between m-ZZ and m-AC chains with the critical stress of 0.65 nN. If an m-ZZ chain is continuously stretched, it approaches, but cannot reach before breakdown, a linear chain geometry around $n = 2.40$ Å. If an m-AC chain is compressed, it emerges a complicated region that m-AC may coexist with high pressure phases d-L and d-ZZ at n round 1.20 Å. As we found in broken symmetry relaxations, m-AC chains may collapse into d-ZZ chains at n in a range of 1.44 Å to 1.22 Å. Similar to the mono-atomic chain case, d-ZZ is the most stable one among all three dual-atomic chains and it could be reversibly transferred to d-AC. All these three dual-atomic chain phases have similar atomic structural blocks to the high-pressure NaCl phase of bulk P crystal. We predict that the d-ZZ, probably d-AC, phase could be created by e-beam from the NaCl phase, which requires the sample holder of an electron microscopy with the capacity of holding a high pressure.

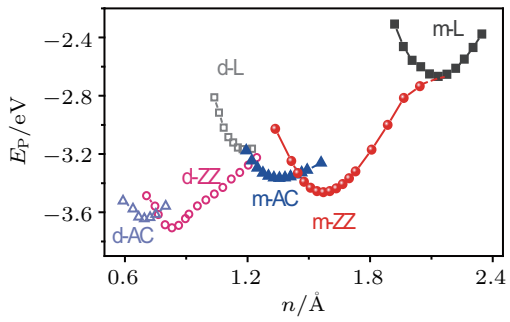


Fig. 2. (color online) Phase diagram of infinite atomic chains shows the relationship between energy and the length per P atom (n). Cube, circle, and triangle are correspondind to linear, zigzag, and armchair chains, respectively. Mono- and dual-atomic chains are indicated by solid and hollow shapes.

3.3. Electronic structures of infinite P chains

Figures 3(a)–3(f) show the electronic band structures of these six infinite atomic chains. Both linear chains are metallic, while d-AC and d-ZZ chains are semiconductor with bandgaps of 0.78 eV and 1.49 eV, respectively. The m-ZZ chain is a special case that it appears as a Dirac semi-metal with the Dirac point at the X point (0.5 0 0) of the BZ. And m-AC is a small-bandgap semiconductor with a bandgap of 0.23 eV. Spin–orbit coupling (SOC) effect was fully included in all bandstructure calculations. Three of them, i.e., m-AC, d-AC, and d-ZZ, do not have appreciable splitting between the two spin components with the consideration of SOC, but the rest show significant separations between the two components. Among those chains having separations, m-L and m-ZZ are of particular interest for the linear dispersion relation and the Dirac-point-like cross in their bandstructures. A zoom-in image of the bandstructure of m-L near the Dirac point is plotted in Fig. 3(g). There are three bands and two spin components, totally six states, available near the crossed points. Spin-splitting occurs between bands L3 (red) and L6 (blue) which are hybridized p_z orbitals reoriented to positive and negative y directions, respectively, as shown by the plots of wavefunction distributions in Fig. 3(g). The reorientation results in a splitting energy of 0.04 eV between these bands with and without SOC. Another feature lies in the appearance of a new type of Dirac point with three-fold degeneracy at the crossed point of higher energy (L6 with L1/2). However, it might not be due to the topological properties of m-L, but might also be a result of

high symmetry of the linear chain. A similarly large splitting energy of 0.06 eV is found in m-ZZ near the Fermi level. Figure 3(h) shows that m-ZZ is a Dirac semi-metal with the Dirac point exactly at X without SOC. However, SOC splits the two spin components, pulling one up and pushing the other down. The Dirac point, therefore, shifts to a point very close to the X point and there is no bandgap opening observed. Both states (ZZ1 and ZZ2) are hybridized p_y states and are slightly reoriented to the positive and negative x directions, respectively. The linear dispersion and semi-metal feathers suggest m-ZZ as a "1D graphene" and imply very high carrier mobility that could be, in principle, measureable in experiments.

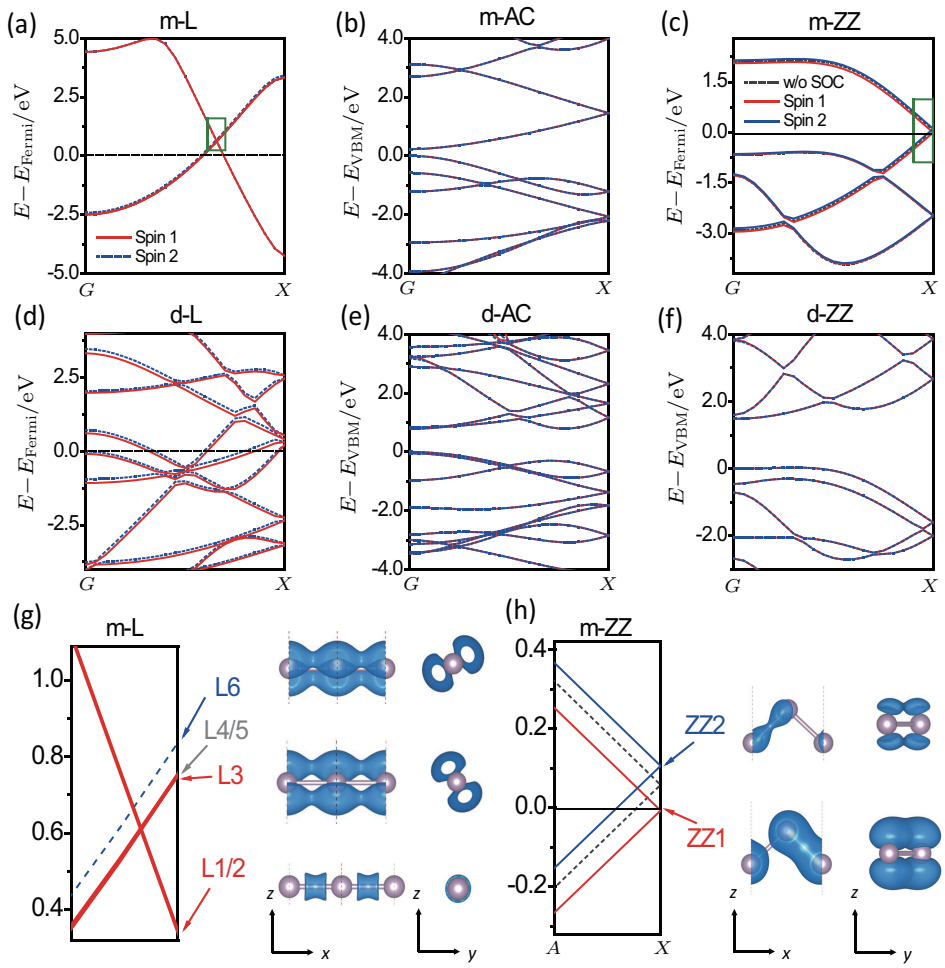


Fig. 3. (color online) Band structures with SOC of infinite m-L (a), m-AC (b), m-ZZ (c), d-L (d), d-AC (e), and d-ZZ (f) chains. Red solid lines and blue dashed or solid lines distinguish two spin components. Black dashed lines in panel (c) indicate the bandstucture of m-ZZ without SOC. Band structures in pannels (g) and (h) are zoom-in plots of green rectangle in pannels (a) and (c), respectively. Three conduction states (L1/2, L3, L6) of m-L are marked in the left pannel of (g). Spatial structures of wavefunctions for the three marked states are shown in the right pannel of (g) using isosurface of 0.005 e·Bohr $^{-3}$. One valence and one conduction states (ZZ1, ZZ2) are marked in the left pannel of (h). Spatial structures of wavefunctions for the two marked states are shown in the right pannel of (h) using isosurface of 0.003 e·bohr $^{-3}$. The coordinates of A and X points are (0.4 0 0) and (0.5 0 0).

3.4. Encapsulated finite P chains

In analog to pioneering studies on atomic chains, e.g., graphene,[5] BN,[7] or MoS_2,[8] mono- or few-atom atomic chains were usually realized as finite chains encapsulated between two nanoribbons. Here, we investigated over 120 configurations of mon- and dual-atomic finite phosphorus chains encapsulated in two BP ribbons with (supported finite chains) and without BP sheets underneath (suspended finite chains). The BP sheets underneath usually stabilize the chain through the chain–sheet, mostly van der Waals, interaction.[35–37] However, even with a BP sheet, supported encapsulated linear, either for mono- or dual-atomic, chains collapse into isolated atoms, atomic clusters, or ZZ chains attaching to the BP sheet, in consistent with the stability orders found in the infinite chains. Finite ZZ chains are, again, the most stable configurations among all finite mono- and dual-atomic chains. Figures 4(a)–4(d) show the atomic structures of the chains with the lowest E_P among their categories for suspended and supported m-ZZ and d-ZZ chains. Their n values, i.e., 1.60 Å, 0.84 Å, 1.60 Å, and 0.84 Å, respectively, differ only 0.01-0.03 Å from those of infinite chains. In terms of other obtained chains with higher E_P, the n value varies from 1.49–1.63 Å and 0.83–0.86 Å for m-ZZ and d-ZZ chains, respectively. In the presence of BP sheets, the m-ZZ chain rotates

90° along the chain axis (Fig. 4(b)) in supported m-ZZ chain, the zigzag pattern of the chain is nearly along the [100] direction of BP maximizing the overlap between the chain atoms and the atoms underneath. This chain–sheet interaction, however, does not result in substantial angle dependence of the chain, which is a result of higher stability and flexibility under stretching and compression of ZZ chains. A very recent electron microscopy experiment also suggests that ZZ chains are more often observed and rather flexible at finite temperature or under electron beam.[34]

Finite AC chains are less stable compared with ZZ chains. However, m-AC chains can be either obtained in suspended or supported forms if n is in a proper range for AC chains, e.g., 1.32–1.40 Å. Figure 4(e) shows the atomic structure for the suspended encapsulated m-AC chain with the lowest E_P. Again, the n values of finite m-AC chains are very close to those found in infinite AC chains. Although the presence of BP sheets as substrate often stabilizes the supported chains, it is, however, not the case for m-AC chains. In a supported m-AC chain, a few P atoms at the ends of the chain are assimilated into edge atoms, leading to a larger effective n value. Therefore, as a result, the m-AC chain transfers into m-ZZ chains. As shown in Fig. 4(f), it prevents such transformation if the chain angle with respect to the ribbon edge is around a certain angle, namely, 37°. This angle is roughly along the [110] direction (∼ 36°) of the BP sheet. In addition, the length of supported m-AC chains also appears to be limited up to 25 Å. These results are consistent with TEM observation of a less often observed category of supported BP chains which have shorter length and angle selectivity of 36°.[34]

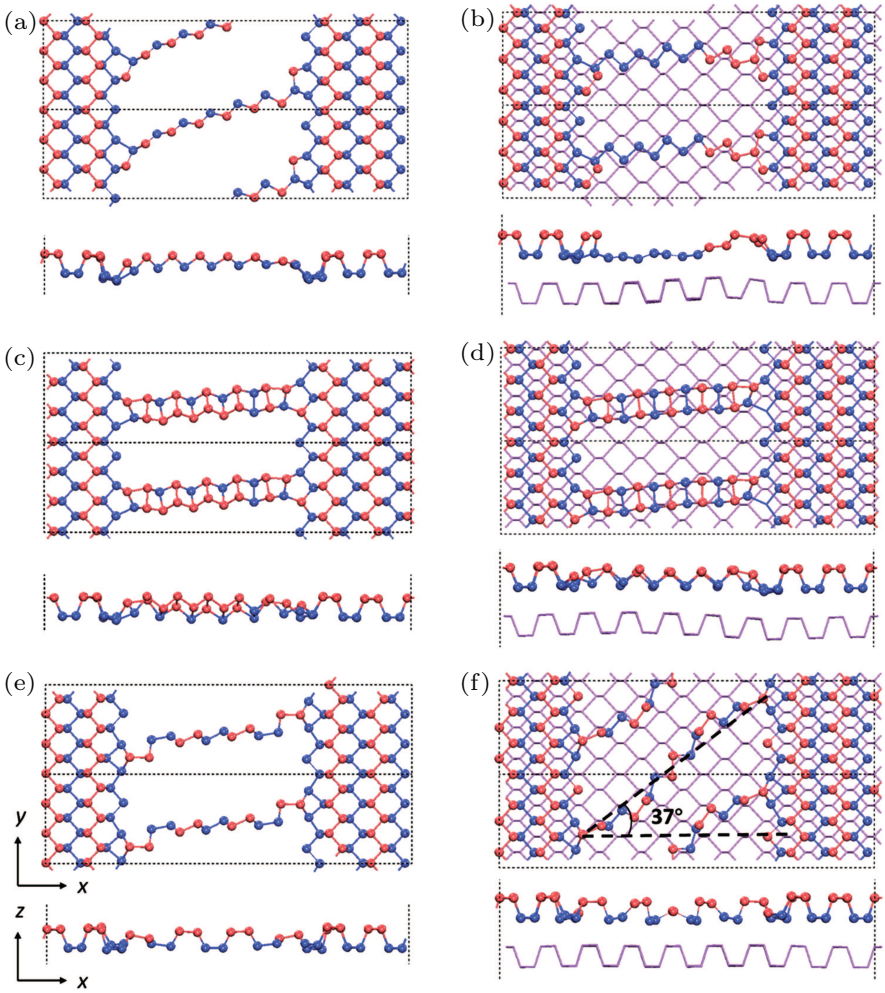


Fig. 4. (color online) Atomic structures of the most stable configuration of suspended ((a), (c), (e)) and supported ((b), (d), (f)) finite m-ZZ ((a), (b)), d-ZZ ((c), (d)), and m-AC chains ((e), (f)).

4. Conclusion and perspectives

In summary, we investigated the geometric stability and electronic properties of infinite, suspended, and supported finite mono- and dual-atomic BP chains. Regardless the width and length of the chain, the zigzag form is always the most energetic stable one and the linear chain is difficult to realize and rather fragile under compression of stretching. As the phase diagram suggested, AC chain can be reversibly transferred to ZZ chain if varying the length density of P atoms, n, from the range of AC chains (1.3–1.4 Å) to that of ZZ chains (1.5–1.6 Å). This range does not substantially change among infinite, suspended, and supported finite chains. Strong

SOC effect is observed in both linear chains and the m-ZZ chain. It turns out that the infinite m-ZZ is most likely a Dirac semimetal with the Dirac point slightly off the X point. In terms of finite chains, m-ZZ is again the most stable one among those three forms. No appreciable angle dependence is found for suspended and supported finite chains except for the supported m-AC chain that it prefers the [110] direction of BP sheet, roughly 35° to 37° with respect to the normal direction of BP. This work reveals the geometric stability of various P atomic chains and shows their transitions from one form to another, especially between AC and ZZ chains. In addition, the fairly stable m-ZZ chain was predicted a Dirac semimetal with extremely high carrier mobility. These results pave the way of extending the world of mono- or few-atom chains from graphene, BN, and TMD to BP, which may promote future research on electronic and optoelectronic properties of BP chains.

Note that during preparing this manuscript, we were aware that likely mono-atomic BP chains were fabricated and observed in a very recent transmission electronic microscope experiment.[34]

Acknowledgment

We are grateful to Chuanhong Jin and Zhangru Xiao for their fruitful communications on experimental observation of finite BP chains. Calculations were performed at the Physics Laboratory for High-Performance Computing of Renmin University of China and at the Shanghai Supercomputer Center.

References

[1] Geim A K and Novoselov K S 2007 *Nat. Mater.* **6** 183
[2] Wang Q H, Kalantar-Zadeh K, Kis A, Coleman J N and Strano M S 2012 *Nat. Nanotechnol.* **7** 699
[3] Xia F, Wang H, Xiao D, Dubey M and Ramasubramaniam A 2014 *Nat. Photon.* **8** 899
[4] Kang S J, Kocabas C, Ozel T, Shim M, Pimparkar N, Alam M A, Rotkin S V and Rogers J A 2007 *Nat. Nanotechnol.* **2** 230
[5] Jin C, Lan H, Peng L, Suenaga K and Iijima S 2009 *Phys. Rev. Lett.* **102** 205501
[6] Chuvilin A, Meyer J C, Algara-Siller G and Kaiser U 2009 *New J. Phys.* **11** 083019
[7] Cretu O, Komsa H P, Lehtinen O, Algara-Siller G, Kaiser U, Suenaga K and Krasheninnikov A V 2014 *ACS Nano* **8** 11950
[8] Liu X, Xu T, Wu X, Zhang Z, Yu J, Qiu H, Hong J H, Jin C H, Li J X, Wang X R, Sun L T and Guo W 2013 *Nat. Commun.* **4** 1776
[9] Lin J, Zhang Y, Zhou W and Pantelides S T 2016 *ACS Nano* **10** 2782
[10] Li L, Yu Y, Ye G J, Ge Q, Ou X, Wu H, Feng D, Chen X H and Zhang Y 2014 *Nat. Nanotechnol.* **9** 372
[11] Qiao J, Kong X, Hu Z X, Yang F and Ji W 2014 *Nat. Commun.* **5** 4475
[12] Liu H, Neal A T, Zhu Z, Luo Z, Xu X, Tománek D and Ye P D 2014 *ACS Nano* **8** 4033
[13] Xia F, Wang H and Jia Y 2014 *Nat. Commun.* **5** 4458
[14] Jia Q, Kong X, Qiao J and Ji W 2016 *Sci. China Phys. Mechan. Astron.* **59** 1
[15] Zhao J, Nam H, Ly T H, Yun S J, Kim S, Cho S, Yang H and Lee Y H 2017 *Small* **13** 1601930
[16] Gunlycke D, Vasudevan S and White C T 2013 *Nano Lett.* **13** 259
[17] Komsa H-P, Kurasch S, Lehtinen O, Kaiser U and Krasheninnikov A V 2013 *Phys. Rev. B* **88** 035301
[18] Vierimaa V, Krasheninnikov A V and Komsa H P 2016 *Nanoscale* **8** 7949
[19] Blochl P E 1994 *Phys. Rev. B* **50** 17953
[20] Kresse G and Joubert D 1999 *Phys. Rev. B* **59** 1758
[21] Kresse G and Furthmuller J 1996 *Phys. Rev. B* **54** 11169
[22] Paolo G, Stefano B, Nicola B, Matteo C, Roberto C, Carlo C, Davide C, Guido L C, Matteo C, Ismaila D, Andrea Dal C, Stefano de G, Stefano F, Guido F, Ralph G, Uwe G, Christos G, Anton K, Michele L, Layla M S, Nicola M, Francesco M, Riccardo M, Stefano P, Alfredo P, Lorenzo P, Carlo S, Sandro S, Gabriele S, Ari P S, Alexander S, Paolo U and Renata M W 2009 *J. Phys.: Condens. Matter* **21** 395502
[23] Baroni S, de Gironcoli S, Dal Corso A and Giannozzi P 2001 *Rev. Mod. Phys.* **73** 515
[24] Lee K, Murrayé D, Kong L, Lundqvist B I and Langreth D C 2010 *Phys. Rev. B* **82** 081101
[25] Dion M, Rydberg H, Schröder E, Langreth D C and Lundqvist B I 2004 *Phys. Rev. Lett.* **92** 246401
[26] Klimeš J, Bowler D R and Michaelides A 2010 *J. Phys.: Condens. Matter* **22** 022201
[27] Klimeš J, Bowler D R and Michaelides A 2011 *Phys. Rev. B* **83** 195131
[28] Zhao Y, Qiao J, Yu P, Hu Z, Lin Z, Lau S P, Liu Z, Ji W and Chai Y 2016 *Adv. Mater.* **28** 2399
[29] Hu Z X, Kong X, Qiao J, Normand B and Ji W 2016 *Nanoscale* **8** 2740
[30] Zhang Y, Qiao J, Gao S, Hu F, He D, Wu B, Yang Z, Xu B, Li Y, Shi Y, Ji W, Wang P, Wang X, Xiao M, Xu H, Xu J B and Wang X 2016 *Phys. Rev. Lett.* **116** 016602
[31] Zhao Y, Luo X, Li H, Zhang J, Araujo P T, Gan C K, Wu J, Zhang H, Quek S Y, Dresselhaus M S and Xiong Q 2013 *Nano lett.* **13** 1007
[32] Li M, Dai J and Zeng X C 2015 *Nanoscale* **7** 15385
[33] Hong J, Hu Z, Probert M, Li K, Lv D, Yang X, Gu L, Mao N, Feng Q, Xie L, Zhang J, Wu D, Zhang Z, Jin C, Ji W, Zhang X, Yuan J and Zhang Z 2015 *Nat. Commun.* **6** 6293
[34] Xiao Z, Qiao J, Lu W, Ye G, Chen X, Zhang Z, Ji W, Li J and Jin C 2017 *Nano Research*
[35] Ji W, Timoshevskii V, Guo H, Abou-Rachid H and Lussier L S 2009 *Appl. Phys. Lett.* **95** 021904
[36] Timoshevskii V, Ji W, Abou-Rachid H, Lussier L S and Guo H 2009 *Phys.Rev. B* **80** 115409
[37] Smeu M, Zahid F, Ji W, Guo H, Jaidann M and Abou-Rachid H 2011 *J. Phys. Chem. C* **115** 10985